Biased reptation of polyampholytes: Trapping and enhancement effects

D. Loomans,[a] H. Schiessel, and A. Blumen
Theoretical Polymer Physics, Freiburg University, Rheinstr. 12, 79104 Freiburg, Germany

(Received 24 March 1997; accepted 13 May 1997)

We consider the dynamics of polyampholytes (PAs, polymers containing positive and negative charges) in a fixed network (gel). Under the influence of an external electrical field a PA undergoes a biased reptation; the electrophoretic mobility of the chain depends crucially on the given charge distribution. This effect, which does not occur for equally charged polymers (polyelectrolytes, e.g., DNA) leads to an effective separation of PAs according to their charge distribution—even for PAs of the same length and the same overall charge. © *1997 American Institute of Physics.* [S0021-9606(97)51531-5]

I. INTRODUCTION

DNA gel electrophoresis is an effective method for separating DNA strands of different lengths.[1,2] This is of great technical importance since polyelectrolytes (PEs) in solution tend to have the same electrophoretic mobility, independent of their number of monomers N: both the electrical force as well as the friction force (DNA are free-draining coils) are proportional to N. The situation where the chains migrate through a gel matrix is different; here already a simple analysis in the framework of the biased reptation model shows the electrophoretic mobility of PEs to follow a $1/N$ dependence, at least for short chains.[3,4] The mobility for longer chains, however, changes as a result of the orientation of the chains in the external field.[4] On the other hand, the biased reptation concept is unable to describe the findings in field-inversion gel electrophoresis (FIGE) where one finds a mobility minimum (''gap'') around some length N. Much work was devoted in recent years to the theoretical understanding of this ''antiresonance'' phenomenon aiming to elucidate the mechanisms underlying FIGE.[5–10]

In this article we extend the considerations for PEs to heterogeneously charged polymers, namely to polyampholytes (PAs); these are heteropolymers which carry both positive and negative charges. In a series of works[11–15] we have investigated how PAs in dilute solutions behave in external electrical fields. As we have shown, PAs stretch strongly in external fields; the details depend on the distribution of charges[12,15] and on their intramolecular coupling,[14,15] on the solvent's quality,[14,15] on the chain's extensibility[13] (cf. also the paper of Winkler and Reineker[16]), and on the hydrodynamic interaction between the monomers.[15] A great variety of static and dynamical scaling laws follow.

We hasten to note that the presence of geometrical constraints can modify strongly the PAs' dynamics in external fields. Thus in Ref. 17 an analysis was performed of collisions of PA chains with static posts; the focus of the investigation was to evaluate the time it takes a PA chain to unhook. It turns out that in general this time depends exponentially on N. This is different from the situation which one finds for PEs, where the time to unhook depends algebraically on N; as a consequence of this one does not achieve a significant separation of PEs through a series of collisions with sparsely distributed hooks.[18]

In this paper we consider a somehow more complicated situation; we study namely the mobility of PAs through fixed, very dense networks. In this case the prevailing geometrical constraints effectively confine the polymer to a tube.[19,20] Due to the densely spaced obstacles, the chain is only allowed to leave the tube by reptating, i.e., by moving as a whole along the tube, creating at one end a new tube segment and erasing such a segment at the other end. As it is well-known, reptation also holds for polymer melts, where the other chains of the melt act as obstacles which are long-lived compared to the tube-engagement time.[19,20] For a charged chain in an electrical field one has further to take into account the external force acting on the polymer; this leads—in the simplest version—to the biased reptation model,[3,4] which was developed in order to model the gel electrophoresis of PE (DNA).

In this work we use a slightly modified version of biased reptation and investigate the PAs' dynamics in not-too-strong fields. Using simple scaling arguments as well as numerical simulations, we show that the mobility of PA chains in dense networks depends strongly on the PAs' distribution of charges, even for PAs with the same degree of polymerization N and total (excess) charge Q_{tot}. Taking a PE chain as a reference, we find, depending on the specific distribution of charges, that the PAs' mobility is sometimes enhanced and sometimes reduced. Thus gel electrophoresis allows the separation of PAs according to specific features of the distribution of charges along the chain.

II. BIASED REPTATION DYNAMICS

Let us now consider PAs in fixed networks (gels) in the framework of biased reptation.[4] As mentioned above, the basic idea is that the embedding medium (network) limits the dynamics of the chain to a tube-like region, i.e., to a reptating motion.[19,20] Due to fluctuations on small scales, the length L of the chain and the contour length of the tube, L_c, are different ($L \geqslant L_c$). Being interested in mesoscopic properties, the small-scale fluctuations of the chain are dis-

[a]Present address: Siemens AG, HL TS E DS, Postfach 80 17 09, 81617 Munich, Germany.

 0021-9606/97/107(7)/2636/7/$10.00

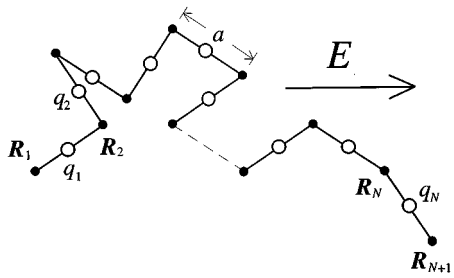

FIG. 1. PA in a fixed network. The PA is represented by its primitive chain with the fixed length $L_c = aN$. Each segment carries the effective charge q_n.

regarded; one represents the PA's conformation by a tube of fixed length L_c, the so-called *primitive chain*.[20] Note, however, that the assumption of constant L_c is valid only for not-too-strong external fields: The deformation energy per segment (of length a) is much smaller than the thermal energy T (expressed in units of the Boltzmann constant k_B), i.e., when

$$aF_{\text{ext}} \ll T. \tag{1}$$

Under this condition the PA is modeled through $N+1$ ''beads'' which are connected into a linear chain by N bonds of fixed length (cf. Fig. 1). The chain has the (fixed) total length $L_c = aN$, where the parameter a is the step length of the primitive chain (and depends on the statistical properties of the network). a and N are related to the bond length b and the degree of polymerization N of the elementary chain through $a^2N = b^2N$. The primitive chain is ''freely jointed,'' i.e., each segment is able to point in any direction independently of the other bonds. The chain's conformation at time t is represented by the set $\{\mathbf{R}_n(t)\}$, where $\mathbf{R}_n(t) = (X_n(t), Y_n(t), Z_n(t))$ denotes the position of the nth bead. Furthermore, the chain carries N charges q_n $(n = 1,...,N)$ located in the middle of each link, i.e., between each pair of neighboring beads; these charges represent the effective charges of the primitive chain segments. Their positions are given by the set $\{\mathbf{r}_n(t)\}$ with $\mathbf{r}_n(t) = (x_n(t), y_n(t), z_n(t))$ $(n = 1,...,N)$ being the position of the charge on the nth segment:

$$\mathbf{r}_n(t) = \tfrac{1}{2}(\mathbf{R}_n(t) + \mathbf{R}_{n+1}(t)). \tag{2}$$

Thus the potential of the chain in the external electrical field is given by

$$U(t) = -\sum_{n=1}^{N} q_n \mathbf{E}\mathbf{r}_n(t). \tag{3}$$

In Eq. (3) the intra- as well as the intermolecular electrostatic interaction of the charged monomers is neglected. This is justified, for instance, for weakly charged, short PA chains. More specifically, for a Θ solvent and a randomly charged PA with vanishing total charge, the coupling between the charges can be neglected as long as $N < (b/fl_B)^2$ holds.[15,21,22] Here f denotes the fraction of charged monomers and $l_B = e^2/(\varepsilon T)$ is the Bjerrum length (with e being the elementary charge per monomer and ε the dielectric constant); in water at room temperature one has $l_B \cong 7$ Å. In terms of the primitive chain, this so-called weak-coupling condition turns into the inequality $N < (a\varepsilon T/q^2)^2$, with q being the typical effective charge per primitive chain segment. In this regime also, multichain effects can be neglected, since then the electrostatic energy per chain is smaller than T (cf. Ref. 23 for a detailed discussion of the role of finite concentrations). These arguments remain valid for non-neutral chains as long as the charge asymmetry is small enough, namely as long as $Q_{\text{tot}} < qN^{1/2}$.[15,24]

Due to the entanglements, the PA is only allowed to move along the tube; we describe the chain's reptation by the following Monte Carlo (MC) method: Assume the PA at time t to have the conformation $\{\mathbf{R}_n(t)\}$. During the time step Δt, the PA attempts to make a forward or backward jump to a new conformation of the form:

$$\mathbf{R}_n^{(\text{trial})}(t+\Delta t) = \tfrac{1}{2}(1+f(t))\mathbf{R}_{n+1}(t) + \tfrac{1}{2}(1-f(t))\mathbf{R}_{n-1}(t), \tag{4}$$

with $1 \leqslant n \leqslant N+1$. Here $f(t)$ is a stochastic variable which takes with equal probability 1/2 the values $+1$ for a forward jump of the chain $(n \to n+1)$ and -1 for a backward jump $(n \to n-1)$. These elementary events are accepted or rejected following the usual Monte Carlo rules: If the potential $U(t+\Delta t)$ of the new trial conformation is energetically more favorable, i.e., if $U(t+\Delta t) \leqslant U(t)$, the new conformation is accepted and one sets $\mathbf{R}_n(t+\Delta t) = \mathbf{R}_n^{(\text{trial})}(t+\Delta t)$. If $U(t+\Delta t) > U(t)$, the new conformation is only accepted with probability $p = \exp(-\Delta U/T)$ (Boltzmann factor); otherwise (with probability $1-p$), $\mathbf{R}^{(\text{trial})}$ is rejected and one sets $\mathbf{R}_n(t+\Delta t) = \mathbf{R}_n(t)$.

Moreover, we have to deal in Eq. (4) with the boundary conditions. When one has a forward (backward) jump the $(N+1)$th (first) bead leaves the tube; the position of this bead, $\mathbf{R}_{N+2}$ $(\mathbf{R}_0)$ in Eq. (4), is then given by

$$\mathbf{R}_{N+2}(t) = \mathbf{R}_{N+1}(t) + \mathbf{a}(t) \tag{5}$$

for a forward jump, or by

$$\mathbf{R}_0(t) = \mathbf{R}_1(t) + \mathbf{a}(t) \tag{6}$$

for a backward jump. In Eqs. (5) and (6), $\mathbf{a}(t)$ represents a random vector of length $|\mathbf{a}(t)| = a$; by this a new, randomly directed section of the tube is created.

Let us note the differences between this model and the original biased reptation model of Slater and Noolandi.[4] In our case we use a Monte Carlo method to determine the next move; we are thus, at least formally, able to handle electrical fields of arbitrary strength. It is a simple matter to show by linearizing the Boltzmann factor that for not-too-strong fields [cf. Eq. (1)] our approach reproduces the formalism of Ref. 4; the bias due to the field can then be directly incorporated into the stochastic properties of $f(t)$ of Eq. (4) (see Ref. 4 for details). A second modification in our approach concerns the creation of new tube segments. In Eqs. (5) and (6) we pick the new segments $\mathbf{a}(t)$ from an isotropic distribution. This is different from Ref. 4, where the new segments are assumed

to get oriented towards the field; for stronger fields this mechanism leads to a stretching of the whole chain. From the point of view of very dense networks, it is, however, questionable whether the geometry allows such a strongly directional orientation of the ends; thus we restrain ourselves from incorporating this effect into the model.

III. ELECTROPHORETIC MOBILITY

In Ref. 3 Lumpkin and Zimm succeeded in determining the electrophoretic mobility of PEs in gels using straightforward concepts. As we proceed to show, the situation for PAs is much more complex, so that simple extensions of these concepts encounter serious limitations. To show this we start from the actual tangential (longitudinal) electric force $F_l(t)$ acting on the polymer along the contour of the tube. For a given tube conformation $\{\mathbf{R}_n(t)\}$, each charged segment n leads to a force contribution along the tube of $q_n\mathbf{E}\cdot(\mathbf{R}_{n+1}(t)-\mathbf{R}_n(t))/a$ (cf. Fig. 1). Hence one has by summing over all contributions (this assumes the chain to be incompressible and inextensible):

$$F_l(t)=\frac{\mathbf{E}}{a}\sum_{k=1}^{N} q_k(\mathbf{R}_{k+1}(t)-\mathbf{R}_k(t)) = \frac{E}{a}\sum_{k=1}^{N} q_k(Y_{k+1}(t)-Y_k(t)), \tag{7}$$

where in the last line (and also in the following) the electrical field is taken to point in the Y direction, i.e., $\mathbf{E}=(0,E,0)$. From Eq. (7) the chain's tangential (longitudinal) drift velocity along the tube is given by $\nu_l(t)=F_l(t)/\zeta_l$, where ζ_l denotes the total translational (longitudinal) friction coefficient of the PA.

This translational motion is accompanied by a drift of the center of mass (c.m.) in the medium which can be calculated as follows:[4] A forward jump may be seen as the transfer of the end segment to the front position where a new part of the chain is generated; this corresponds approximately (within a accuracy of order $1/N$) to moving this segment over the distance $\mathbf{P}(t)=\mathbf{R}_{N+1}-\mathbf{R}_1$. Obviously a backward jump may be seen as the transfer of a segment approximately over the distance $-\mathbf{P}(t)$. Thus the change $\Delta_{\pm}\mathbf{R}_{\text{c.m.}}(t)$ of the position of the c.m. $\mathbf{R}_{\text{c.m.}}(t)$, for a forward/backward jump is given by

$$\Delta_{\pm}\mathbf{R}_{\text{c.m.}}(t)\cong f_N\frac{\pm\mathbf{P}(t)}{N}. \tag{8}$$

In Eq. (8) we have introduced the factor $f_N=(N-1)/N$ which takes into account that the transfer distance of the end segment is effectively smaller than $\pm\mathbf{P}(t)$: During a reptation step, one segment of the chain with a typical length of $\mathbf{P}(t)/N$ vanishes, whereas the new part of the tube has a random orientation [cf. Eqs. (5) and (6)]. Now, the CM's drift velocity in the Y direction at time t, $\nu^Y_{\text{c.m.}}(t)$, follows from the tangential drift velocity $\nu_l(t)$ along the tube. Using Eq. (8) one finds

$$\nu^Y_{\text{c.m.}}(t)\cong\frac{f_N P_Y(t)}{aN}\,\nu_l(t), \tag{9}$$

with $P_Y(t)$ being the Y component of $\mathbf{P}(t)$.

Here we are interested in the *electrophoretic mobility* $\mu(E)=\overline{\nu^Y_{\text{c.m.}}}/E$ where $\overline{\nu^Y_{\text{c.m.}}}$ denotes the average drift velocity of the c.m. Hence we take that $\overline{\nu^Y_{\text{c.m.}}}$ is given by the time average $\langle\ldots\rangle$ of Eq. (9) so that:

$$\mu(E)=\langle\nu^Y_{\text{c.m.}}\rangle/E=\frac{f_N}{a^2N\zeta_l}\sum_{k=1}^{N} q_k\langle(Y_{k+1}-Y_k)P_Y\rangle. \tag{10}$$

As we will see, Eq. (10) often overestimates the PA's mobility.

In the following we discuss three different kinds of charged polymers: PEs, diblock, and triblock PAs. Even letting each polymer carry the same total charge Q_{tot}, we find vastly different behaviors for the three classes: For small external fields E the mobility of PEs is essentially constant, whereas the mobilities of the diblock and triblock PAs increase and decrease with E; for larger E we observe additional effects. In the following we present the three cases separately.

A. Polyelectrolytes

Let us consider first a homogeneously charged PE with $q_n=\Delta q$ for $n=1,\ldots,N$; the chain's total charge is thus given by $Q_{\text{tot}}=N\Delta q$. From Eq. (10) we find for the electrophoretic mobility of the PE:

$$\mu(E)=\frac{f_N Q_{\text{tot}}}{a^2N^2\zeta_l}\langle P_Y^2\rangle. \tag{11}$$

For small field strengths [cf. Eq. (1)], field-induced changes of the conformation are small and the reptating chain will be, by construction, nearly Gaussian. Then $\langle P_Y^2\rangle=a^2N/3$, which leads with Eq. (11) to the result of Refs. 3 and 4:

$$\mu(E)=\frac{f_N Q_{\text{tot}}}{3N\zeta_l}\equiv\mu_N, \tag{12}$$

which is now independent of E. Furthermore, since both Q_{tot} and ζ_l are proportional to N, one finds for small E that the electrophoretic mobility is proportional to N^{-1}.

Using the Monte Carlo method described above we recover this result. In Fig. 2 we depict the simulation results for a PE chain of length $N=24$ and a charge $q_n=\Delta q=0.05$ on each monomer. The filled circles show the rescaled mobility $\mu^{(\text{MC})}(E)/\mu_N$ at different field strengths E; for each E value $\mu^{(\text{MC})}(E)$ denotes the average over ten realizations of 10^7 Monte Carlo steps. For the simulations we have to relate the time Δt for an elementary Monte Carlo event [cf. Eq. (4)] to the longitudinal friction coefficient ζ_l. This is best done for $E\equiv 0$, when each elementary step is accepted. Now the friction coefficient follows from the longitudinal diffusion coefficient through the Einstein relation $\zeta_l=T/D_l$; for the longitudinal (effectively one-dimensional) diffusion with step length a, D_l is given by $D_l=a^2/(2\Delta t)$. Thus we can identify ζ_l with $2\Delta T/a^2$, and Eq. (12) takes the form $\mu_N/f_N=a^2\Delta q/(6\Delta tT)$. In the simulation we set T

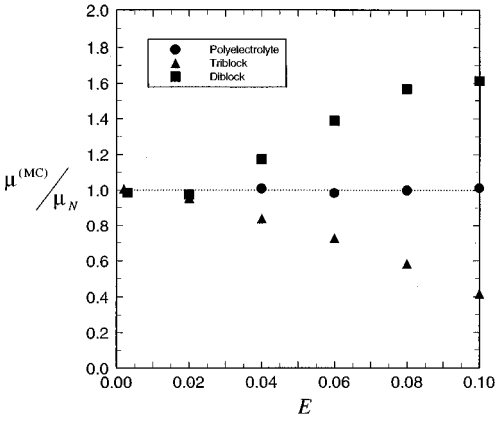

FIG. 2. Electrophoretic mobility $\mu(E)$ of charged polymers with three different kinds of charge distributions for small external fields. Depicted is the relative electrophoretic mobility $\mu^{(\mathrm{MC})}(E)/\mu_N$ as a function of E for a polyelectrolyte chain, a triblock PA, and a diblock PA (see text for details).

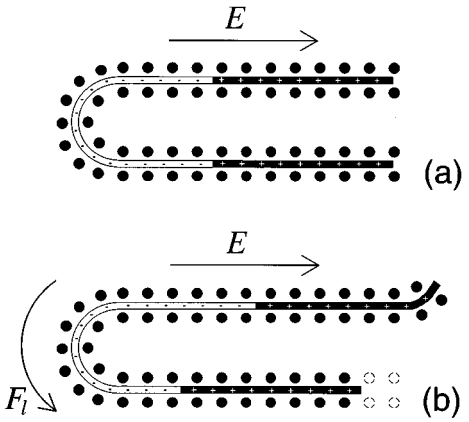

FIG. 3. Triblock PA in a network. Schematically depicted is a U-like configuration (the filled circles symbolize the gel fibers). The symmetric U-conformation (a) is locally stable: When the chain leaves the conformation by reptation the longitudinal force F_l immediately counteracts this process [cf. (b)].

$=1$, $a=1$, and $\Delta t=N$ so that here $\mu_N/f_N=0.05/144=1/2880$. Equation (12) predicts $\mu(E)/\mu_N=1$, which is shown in Fig. 2 as a straight line; as can be seen, this agrees very well with the averaged $\mu^{(\mathrm{MC})}(E)/\mu_N$ obtained from the MC simulations (filled circles).

In the following we study the biased reptation of PAs with prescribed charge distributions $\{q_n\}$. Each monomer carries in addition to the small charge Δq a charge $+q$ or $-q$, each type occurring $N/2$ times; furthermore we choose q such that $q \gg \Delta q$. Thus these PAs have again the total charge $Q_{\mathrm{tot}}=N\Delta q$, and for these PAs the PE just discussed serves as a reference chain.

B. Triblock PAs

As a first example we consider the following triblock PA: we take $q_n=q+\Delta q$ for $n=1,...,N/4$, $q_n=-q+\Delta q$ for $n=N/4+1,...,3N/4$, and $q_n=q+\Delta q$ for $n=3N/4+1,...,N$. Here we set $q=1$ and use the same values for the other parameters as for the PE case. In Fig. 2 the filled triangles display the electrophoretic mobility of the triblock PA for different field strengths. For E close to zero, the mobility of the triblock chain starts with the same value as the PE, μ_N; with increasing external field the mobility goes down, and attains its half value $\mu(E)=\mu_N/2$ at a field strength of around $E\approx 0.09$.

The decrease of μ with E can be understood as follows. In the triblock case there often occur conformations in which the chain becomes trapped. Such a typical U-conformation of low energy is depicted schematically in Fig. 3(a). Due to the tube confinement the chain can leave this conformation only by reptating; then one arm becomes longer whereas the other shortens [cf. Fig. 3(b)]. The electrical longitudinal force F_l immediately counteracts this process and drives the PA back to the symmetric U-conformation. As long as the chain is trapped in the U-conformation the mobility vanishes. Since this effect is more pronounced for larger E values, the mobility is a decreasing function of E.

To express this effect quantitatively is difficult. First one may try to apply Eq. (10) also to the triblock chain. We have compared our numerical $\mu^{(\mathrm{MC})}(E)$ results with Eq. (10), where we used for Y_k and P_Y also the MC results (averaged over each MC step). We find that the mobilities predicted by Eq. (10) are significantly smaller than the values attained from the direct simulations, i.e., $\mu^{(\mathrm{MC})}(E)$. Thus Eq. (10) does not hold for triblock PAs. We give here an example where this can be seen explicitly. Consider the U-conformation depicted in Fig. 3: The chain may be trapped in this conformation for a long time, just wriggling around the symmetric case (a) and attaining from time to time, due to thermal agitation, unsymmetric conformations [like the conformation depicted in Fig. 3(b)]. Clearly, as long as the chain is trapped in this U-conformation, the PA has a vanishing mobility, i.e., $\mu^{(\mathrm{MC})}\equiv 0$. On the other hand, consider Eq. (10): A straightforward analysis shows that $\mu(E)=0$ for symmetric U-conformations and $\mu(E)<0$ for asymmetric ones. Thus as long as the PA is trapped in the U-conformation the averaged $\mu(E)$ from Eq. (10) is negative, in contradiction to $\mu^{(\mathrm{MC})}\equiv 0$.

In the following, we determine an approximate formula for the mobility of the triblock chain using the theory of activation processes. Assume that the electrical field is small enough so that the typical deformation of the chain is linear in the external force; the chain will lower its potential energy by attaining a U-like conformation, and this energy can be evaluated by considering the two halves of the chain separately. Each half is divided into two halves itself, one half carrying the $N/4$ charges $+q$ and the other half carrying $N/4$ charges $-q$. In the external field E, both halves of the chain will be stretched by a force F_S of the order of $q(N/4)E$, which leads, against the entropic forces, to a deformation $\Delta L\approx a^2(N/2)F_S/T\approx a^2qE(N/2)(N/4)/T$.[19] The deformation is accompanied by a shift of the positive and negative charges against each other so that the potential energy of the triblock PA is lowered by $\Delta U\approx$

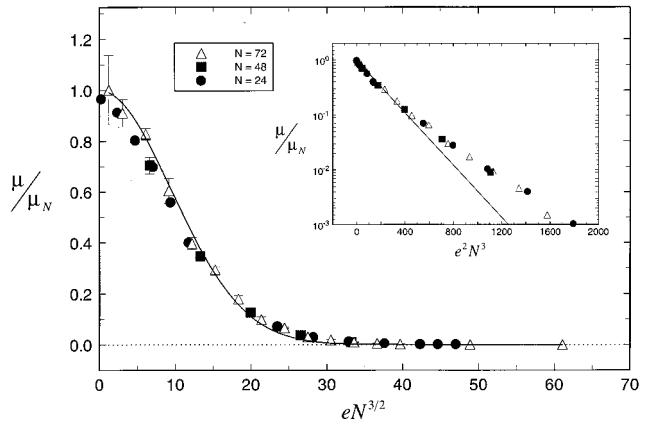

FIG. 4. Reduced plot of the electrophoretic mobility of the triblock PA. The relative electrophoretic mobility μ/μ_N is plotted as a function of $eN^{3/2}$ for three different values of N. Further, we depict the theoretical formula, Eq. (13), as a continuous curve. The inset displays $\ln(\mu/\mu_N)$ as a function of e^2N^3 together with Eq. (13), which is now represented by a straight line. For stronger fields a deviation of the numerical data from the line is observed.

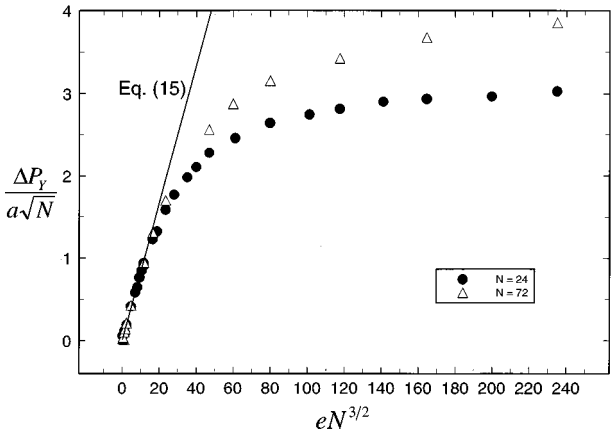

FIG. 5. Field-induced stretching of diblock PAs. Depicted is the relative stretching of the end-to-end distance $\Delta P_Y/(a\sqrt{N})$ as a function of $eN^{3/2}$ for PA chains, with $N=24$ and $N=72$ as well as (straight line) the theoretically predicted curve Eq. (15) (see text for details).

$-2q(N/4)E\Delta L \approx -4a^2q^2E^2(N/4)^3/T$. Assuming further that the electrophoretic mobility scales like $\mu(E) \propto \tau_e^{-1}$, where τ_e is the typical escape time $\tau_e \propto \exp(\Delta U/T)$ from the trapped conformation, we find the following approximate formula for the mobility

$$\mu(E) = \mu_N \exp[-c_1 a^2 q^2 E^2 N^3/T^2]. \tag{13}$$

In Eq. (13) the prefactor is taken to be μ_N (so that $q \to 0$ recovers the PE case); furthermore c_1 is some positive constant.

Equation (13) suggests that $\mu(E)/\mu_N$ is a function of $eN^{3/2}$, with

$$e = aqE/T \tag{14}$$

being the dimensionless field strength. The corresponding rescaled plot, μ as a function of $eN^{3/2}$, is shown in Fig. 4. As can be seen from the figure, the data for different N collapse to a master curve. We also display in Fig. 4, Eq. (13), where we set $c_1 = 0.0055$ in order to fit the simulation results. As can be seen, for not-too-large e, Eq. (13) fits quite well. On the other hand (see insert of Fig. 4), for values of $eN^{3/2}$ larger than 200, the numerical data deviate from Eq. (13).

Let us compare Eq. (13) to the typical unhook time τ_u of a triblock PA which collides with a cylindrical post.[17] In this case we found that $\tau_u^{-1} \propto \exp(-ca^2qQ_{\rm tot}E^2N^2/T^2)$ where c is a positive constant. Note that for single hook collisions (in contrast to the reptation case) the total charge enters into the exponential factor.

C. Diblock PAs

We turn now to the following diblock PA: $q_n = q + \Delta q$ for $n = 1,...,N/2$ and $q_n = -q + \Delta q$ for $n = N/2+1,...,N$, and use the same parameters as for the triblock PA. In Fig. 2 the mobility $\mu(E)$ of the diblock chain is displayed through filled squares. Evidently, for extremely low fields, $E \to 0$, the diblock PA has the same mobility as the PE: Contrary to the triblock PA case, however, the mobility of the diblock PA increases with increasing E. This enhancement can be understood by the fact that it is energetically favorable for the diblock PA to stretch in the direction of the field. Thus we may assume that for not-too-strong fields, $\langle P_Y^2 \rangle$ is given by the corresponding value of a PA chain in a dilute solution:

$$\langle P_Y^2 \rangle = \frac{a^2N}{3} + \frac{a^4q^2E^2N^4}{144T^2}, \tag{15}$$

[cf. Eq. (25) of Ref. 15]. Now we use, tentatively, Eq. (10) again. The symmetry of the deformation with respect to the middle of the chain leads us immediately to Eq. (11). Replacing $\langle P_Y^2 \rangle$ in Eq. (11) by Eq. (15) we end up with

$$\mu(E) = \mu_N + \frac{f_N Q_{\rm tot} a^2 q^2 N^2}{144 \zeta_l T} E^2 = \mu_N \left(1 + \frac{a^2 q^2 N^3 E^2}{48 T^2} \right). \tag{16}$$

Equation (16) predicts an increase of the mobility with increasing E which results from the stretching of the chain. This is contrary to the triblock case: Here the chain in a dilute solution shows no stretching in the field due to the symmetric halves of the chain, and one finds $\langle P_Y^2 \rangle = b^2N/3$ independently of the field strength.

Let us compare Eqs. (15) and (16) with our simulation results. The field-induced stretching $\Delta P_Y = \langle P_Y \rangle$ is given by $\Delta P_Y = a^2qEN^2/(12T)$, which corresponds to the second term on the right-hand side of Eq. (15). In Fig. 5 we compare this theoretical prediction with the chain stretching which we find in our simulations. We display the relative stretching $\Delta P_Y/(aN^{1/2})$ as a function of $eN^{3/2}$. For $eN^{3/2} < 20$ the data for different N, as well as the theoretical curve, coincide. For larger field strength one finds, however, that the numerically determined extension falls below Eq. (15). Furthermore, the N-dependence changes, so that the result for different values of N do not scale with $eN^{3/2}$. Note, however, that this behavior is not simply due to the finite extensibility of the chain; this alone would lead to a much larger extension $\Delta P_Y = aN$ at very large external fields (a detailed discussion

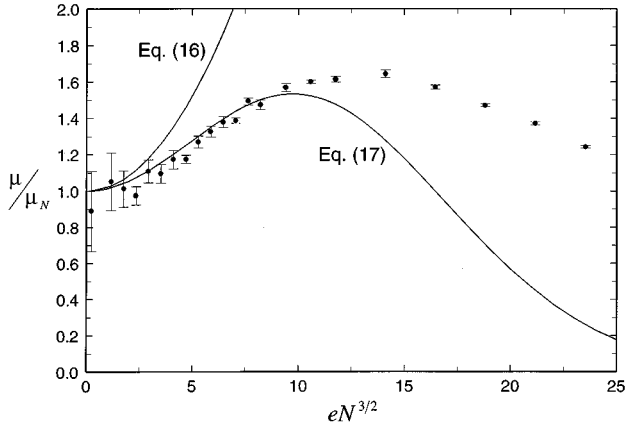

FIG. 6. Electrophoretic mobility of the diblock PA with $N=24$. The numerical results are plotted, together with two approximate formulas (see text for details).

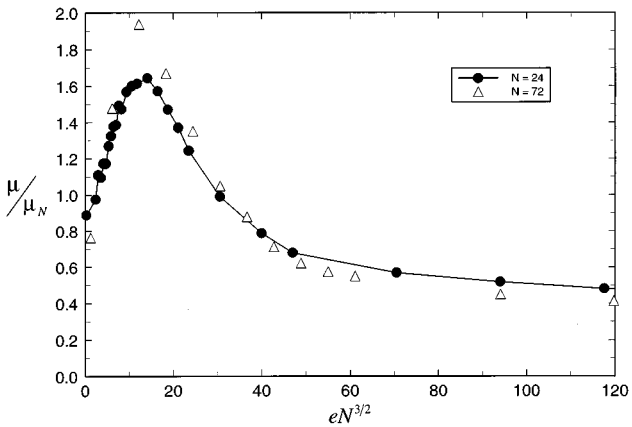

FIG. 7. Electrophoretic mobility of diblock PAs with $N=24$ and $N=72$. Depicted is the relative mobility μ/μ_N as a function of $eN^{3/2}$. Note the scaling of the data for different N.

of the role of the finite extensibility in the case of dilute solutions can be found in Ref. 13). In Fig. 6 we compare the mobility of a diblock PA with $N=24$ with the theoretical curve, Eq. (16). As is evident from the figure, Eq. (16) overestimates the mobility of the diblock chain. The numerical results show a remarkable effect at large e-values: At $eN^{3/2} \approx 14$ the mobility reaches a maximum; for larger values of e the mobility decreases monotonically with the field strength.

Equation (16) is based on the assumption of ergodicity; namely, that in spite of the tube confinement the chain can change from one given configuration to another without being hindered by large potential barriers. This is only the case for sufficiently small fields E. At stronger fields (as in the triblock case), trapping effects occur and the mobility decreases with E. This can be understood as follows: Compared to a stretched conformation a typical random (Gaussian) conformation is energetically less favorable. From Eq. (15) one finds that the energy of the stretched state is lowered by $\Delta U \approx -\Delta P_Y qNE \approx -a^2N^3q^2E^2/T$. For $|\Delta U|>T$, i.e., for field strength $E>E_0$ with $E_0 \approx T/(aqN^{3/2})$, the chain can get trapped into such energetically favorable stretched configurations. We infer that for $E \gtrsim E_0$ the trapping mechanism comes into play and influences the dynamics. We argue now as in the case of triblock PAs and expect an Arrhenius-type correction to $\mu(E)$. This leads to

$$\mu(E)=\mu_N\left(1+\frac{a^2q^2N^3E^2}{48T^2}\right)\exp(-c_2a^2q^2E^2N^3/T^2), \tag{17}$$

where c_2 is a positive constant. The maximal mobility $\mu_{\max}$ of the chain is given for some $E=E_0>0$ as long as c_2 is sufficiently small, namely $c_2<1/48$. Then one has $E_0 = \sqrt{c_2^{-1}-48}T/(aqN^{3/2})$ and $\mu_{\max}=\mu_N(48c_2)^{-1}\exp(48c_2-1)$.

For the sake of comparison, we also display in Fig. 6 Eq. (17) for $c_2=0.007$. Note that for small values of E this description is reasonable. One may also note that trapping influences the mobility even for very small fields, since from Eq. (17) one has $\mu(E)/\mu_N \cong 1+(48^{-1}-c_2)e^2N^3$. This may explain the deviations between Eq. (16) and the numerical data which occur in the limit of small fields (cf. Fig. 6). On the other hand, as can be seen from Fig. 6, for $eN^{3/2}>8$ the decrease of μ which follows from Eq. (17) is much faster than what the numerical data suggest. This deviation may be understood as being due to other pathways by which the chain can leave the energetically favorable configuration.

In Fig. 7 we display the numerical results for the diblock PA's mobility when also very high external fields ($eN^{3/2}$ up to 120) are included. Interestingly, around $eN^{3/2}\approx 50$ a very slow decrease of μ sets in. Furthermore, this large range of E-values allows us to test scaling with respect to $eN^{3/2}$: the normalized values $\mu(E)/\mu_N$ plotted against $eN^{3/2}$ should collapse. We have evaluated these quantities for $N=24$ and $N=72$. Figure 7, where these data are displayed, confirms good scaling for all e considered, even for such e-values for which Eq. (17) does not hold. This suggests that the mobility is of the form $\mu(E)=\mu_N f(eN^{3/2})$, where, following Eq. (17), the function f obeys $f(x)\cong(1+x^2/48)\exp(-c_2x^2)$ for small x, whereas for large values of the argument, f is a very slowly decaying function.

IV. CONCLUSION

In this work we have investigated the motion of PA chains in dense gels and showed (in the framework of biased reptation) that the chains' mobilities depend very strongly on their charge distribution: Chains with the same number of segments N and the same total (excess) charge may display drastically different behaviors, depending on their particular charge distribution. Thus in small external fields the mobility of diblock (triblock) PAs increases (decreases) with the field strength. Furthermore, we showed that ideas developed for PEs cannot be easily extended to PAs. Thus Eq. (10), which is very useful in describing the mobility of PEs [cf. Eq. (12)], does not carry over to PAs; for PAs it is necessary to take account of trapping effects into favorable configurations, whose description requires concepts from the theory of acti-

vation processes. Through a combination of both approaches we were led here to a qualitative understanding of the numerical results.

ACKNOWLEDGMENTS

The authors are indebted to Dr. I. M. Sokolov for fruitful discussions. The support of the DFG (through SFB 428) and of the Fonds der Chemischen Industrie is gratefully acknowledged.

[1] B. Nordén, C. Elvingson, M. Jonsson, and B. Åkerman, Q. Rev. Biophys. **24**, 103 (1991).
[2] B. H. Zimm and S. D. Levene, Q. Rev. Biophys. **25**, 171 (1992).
[3] O. J. Lumpkin and B. H. Zimm, Biopolymers **21**, 2315 (1982).
[4] G. W. Slater and J. Noolandi, Biopolymers **25**, 431 (1986).
[5] B. H. Zimm, J. Chem. Phys. **94**, 2187 (1991).
[6] T. A. J. Duke and J. L. Viovy, J. Chem. Phys. **96**, 8552 (1992).
[7] D. Loomans and A. Blumen, Macromol. Symp. **81**, 101 (1994).
[8] D. Loomans, I. M. Sokolov, and A. Blumen, Macromol. Theory Simul. **4**, 145 (1995).
[9] C. Disch, D. Loomans, I. M. Sokolov, and A. Blumen, Electrophoresis **17**, 1060 (1996).
[10] D. Loomans, I. M. Sokolov, and A. Blumen, Macromolecules **29**, 4777 (1996).
[11] H. Schiessel, G. Oshanin, and A. Blumen, J. Chem. Phys. **103**, 5070 (1995).
[12] H. Schiessel, G. Oshanin, and A. Blumen, Macromol. Theory Simul. **5**, 45 (1996).
[13] H. Schiessel and A. Blumen, J. Chem. Phys. **104**, 6036 (1996).
[14] H. Schiessel and A. Blumen, J. Chem. Phys. **105**, 4250 (1996).
[15] H. Schiessel and A. Blumen, Macromol. Theory Simul. **6**, 103 (1997).
[16] R. G. Winkler and P. Reineker, J. Chem. Phys. **106**, 2841 (1997).
[17] H. Schiessel, I. M. Sokolov, and A. Blumen, Phys. Rev. Lett. (submitted).
[18] G. I. Nixon and G. W. Slater, Phys. Rev. E **50**, 5033 (1994).
[19] P. G. de Gennes, *Scaling Concepts in Polymer Physics* (Cornell University Press, Ithaca, 1979).
[20] M. Doi and S. F. Edwards, *The Theory of Polymer Dynamics* (Clarendon, Oxford, 1986).
[21] P. G. Higgs and J. F. Joanny, J. Chem. Phys. **94**, 1543 (1991).
[22] A. V. Dobrynin and M. Rubinstein, J. Phys. II (France) **5**, 677 (1995).
[23] R. Everaers, A. Johner, and J.-F. Joanny, Europhys. Lett. **37**, 275 (1997).
[24] Y. Kantor, M. Kardar, Phys. Rev. E **51**, 1299 (1995).